

Functional connectivity between areas involved in emotion and executive control is abnormal in patients with psychogenic non-epileptic seizures

S. J. van der Kruijs¹, M. J. Vaessen², N. M. Bodde¹, R. H. Lazon¹, P. A. Hofman², W. H. Backes², A. P. Aldenkamp¹, and J. F. Jansen²

¹Epilepsy Center Kempenhaeghe, Heeze, Netherlands, ²Radiology, Maastricht University Medical Center, Maastricht, Netherlands

Introduction

Psychogenic non-epileptic seizures (PNES) superficially resemble epileptic seizures as they constitute of episodes of altered motor, sensory, and mental function. However, they are not accompanied by epileptiform brain activity [1]. Most PNES patients are initially misdiagnosed as having epilepsy. Misdiagnosis has serious consequences for the patient, such as exposure to unnecessary anticonvulsant medication, and considerable delay to start the appropriate psychological therapy. Structural MRI is not sensitive enough for the diagnosis of PNES. There are indications that the tendency to dissociate is an important predisposition factor for PNES. We investigated whether functional MRI (task related and resting state) could identify biomarkers of brain alterations associated with dissociation in PNES.

Material and Methods

Patients The study population included 11 patients with PNES (6F, 5M, age 34 ± 11 , number of seizures in previous month 2 ± 3), and 13 healthy volunteers (8F, 5M, age 33 ± 11). Intelligence was tested using the Raven's Matrices test, and dissociation screening lists were administered (Dissociation Questionnaire [DISQ], Dissociative Experiences Scale [DES], and Somatoform Dissociation Questionnaire [SDQ]). **fMRI** Imaging was performed at 3.0-Tesla (Philips Achieva). For anatomic reference, first T1-weighted three-dimensional (3D) turbo field echo (TFE) images were acquired with the following parameters: repetition time (TR) 8.2 ms, echo time (TE) 3.7 ms, flip angle 8° , matrix 240×240 , field of view (FOV) $256 \times 256 \times 180 \text{ mm}^3$, 1 mm adjacent coronal slices. Functional MRI data were acquired using a whole-cerebrum single-shot multi-slice BOLD EPI sequence, with TR 2 s, TE 35 ms, flip angle 90° , voxel size $2 \times 2 \times 4 \text{ mm}^3$, matrix 128×128 , 32 contiguous slices per volume, 195 volumes per acquisition. The fMRI paradigms consisted of 4 scans: i) resting state fMRI (rsfMRI) session 1, ii) picture encoding [2], iii) Stroop color naming [3], and iv) rsfMRI session 2. Picture encoding (with high sentimental value; old versus new) was selected for activation of the hippocampus and surrounding areas, and Stroop color-naming (activation versus rest) was selected for activation of the prefrontal network. For the resting state fMRI sessions, subjects were instructed to think of nothing in particular. The rationale to include a 2nd resting state session was that PNES patients often experience seizures during rest following effort. **Analysis** fMRI data analysis was performed in SPM8 routines in Matlab. All images were co-registered, spatially normalized to MNI space, and smoothed (kernel = 8 mm). Activation maps for the task-related paradigms (encode and Stroop) were calculated using standard procedures. A standard random-effects analysis was performed to assess differences between the PNES and control groups. Subsequently, regions of interest with strong activation were defined (of approx. 200 voxels), based on the activation patterns averaged over all subjects. These masks were created in MRIcro. For the rsfMRI analysis [4], each dataset was low-pass-filtered using a finite impulse response filter to remove the effect of high-frequency noise ($f \leq 8.3 \text{ mHz}$). Also, the six motion correction parameters were included in the design matrix as confounders. Seed time courses for each region and subject then were generated, by averaging the signal within the ROI at each time point. Each seed time course then was regressed against all brain voxel time courses to obtain a functional connectivity map, subsequently transformed using the Fisher-Z transformation. Multiple regression was then performed with subject type (patient or control) and session (1 or 2) as covariates. The resulting contrasts were thresholded at the $p < 0.05$ level (corrected for multiple comparisons using regional FDR [5]). Additionally, differences in characteristics between patients with PNES and healthy volunteers were assessed using parametric Student's t- and non-parametric Mann-Whitney U tests. Results are mean \pm standard deviation.

Results

The patients displayed significantly lower intellectual performance (Raven # correct: 44 ± 7 vs 53 ± 3 [ctrl], $p < 0.001$), and significantly higher dissociation ((DES: 1.7 ± 1.18 vs 0.8 ± 1.01 , $p = 0.016$), (DISQ: 1.6 ± 0.24 vs 1.3 ± 0.24 , $p = 0.023$), and (SDQ: 26.1 ± 4.76 vs 21.8 ± 6.66 , $p < 0.001$)). The random-effects analysis did not reveal any significant differences between the picture encoding and Stroop color-naming activation maps between controls and patients with PNES. For the correlation map analysis, 5 ROIs were created: i) left parahippocampus (based on the encode paradigm), ii) right parahippocampus (based on the encode paradigm), iii) inferior precentral sulcus, iv) cingulate sulcus, and v) supramarginal gyrus (based on Stroop). The functional connectivity maps based on seed regions iii (Figure 1) and v (Figure 2) yielded significant group differences in connectivity values. Compared to controls, patients had significantly higher functional correlations between the pre-motor cortex (precentral sulcus) and the cingulate cortex (cingulate gyrus) (average Fisher-Z transformed connectivity values: 0.40 ± 0.13 vs 0.21 ± 0.13 [ctrl]; Figure 1), and between the parietal lobe (supramarginal gyrus) and the insular cortex (insula) and parietal lobe (parieto-occipital fissure) (connectivity values: 0.37 ± 0.21 vs 0.09 ± 0.17 and 0.38 ± 0.23 vs 0.11 ± 0.12 , respectively; Figure 2). Contrast between rsfMRI sessions 1 and 2 was not significant.

Discussion

The PNES patients displayed a higher tendency to dissociate, which may be negatively related to their intelligence [6]. This rsfMRI study yields some interesting functional connections, which are significantly stronger in patients with PNES than in controls. A correlation was observed between the precentral sulcus, which resides in the motor cortex controlling voluntary muscle movement [7], and the cingulate cortex, which is part of the limbic system, involved with emotion formation [7]. Additionally, strong correlations were found between the parietal lobe, which integrates sensory information [7], and the insular cortex, which is linked to perception and emotion [7]. An abnormal strong connection between these regions (involved in emotion, executive control, and movement) hints at an underlying dissociation mechanism where an emotional state can influence executive control, resulting in altered motor function. This behavior is typically observed in patients with PNES during their involuntary seizures.

Conclusion

Resting state fMRI in patients with PNES reveals a connectivity abnormality between areas involved in emotional responses and cognitive integration systems, which could explain the involuntary dissociative states typically seen in patients with PNES.

References

[1] Bodde NM, Clin Neurol Neurosurg. 2009;111(1):1; [2] Deblaere K, Radiology 2005;236(3):996; [3] MacDonald A, Science 2000;288(5472):1835; [4] Waites A, Ann Neurol 2006;59:335; [5] Langers D, Neuroimage 2007;38(1):43; [6] Gudjonsson GH, Br J Psychiatry 1983;142:35; [7] Blakemore & Frith 2000, The Learning Brain. Blackwell Publishing.

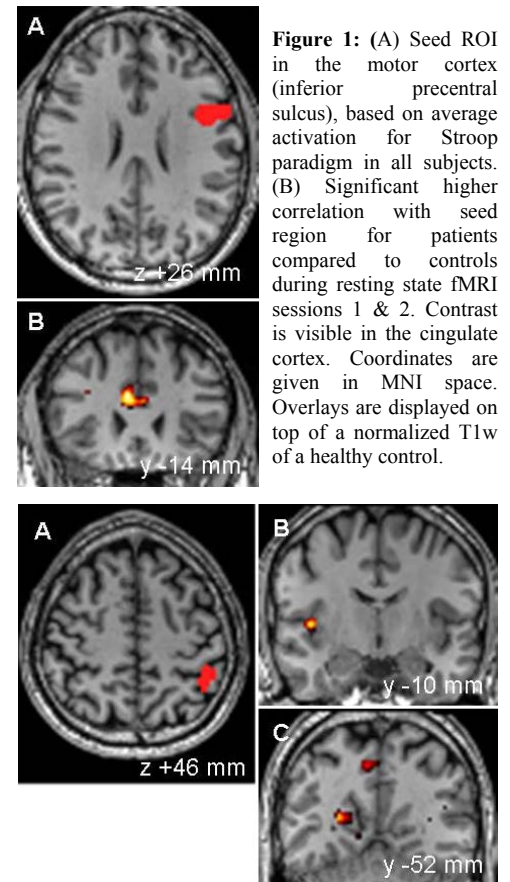


Figure 1: (A) Seed ROI in the motor cortex (inferior precentral sulcus), based on average activation for Stroop paradigm in all subjects. (B) Significant higher correlation with seed region for patients compared to controls during resting state fMRI sessions 1 & 2. Contrast is visible in the cingulate cortex. Coordinates are given in MNI space. Overlays are displayed on top of a normalized T1w of a healthy control.

Figure 2: (A) Seed ROI in the parietal lobe (supramarginal gyrus). Contrast is visible in the insula (B) and the parieto-occipital fissure, medial part (C).